

Application of Artificial Intelligence Techniques for Modeling and Simulation of Photovoltaic Arrays

Mohammad Almomani¹, Ali S. Al-Dmour^{*2}, Seba Algharaibeh³

^{1, 2, 3} Electrical Engineering Department, Mutah University, Karak, Jordan
E-mail: aldmourali2016@gmail.com

Received: July 25, 2020

Revised: September 26, 2020

Accepted: September 29, 2020

Abstract – A method for modeling photovoltaic (PV) arrays - based on artificial intelligence techniques, namely genetic algorithm (GA) and cuckoo optimization algorithm (COA) - is presented. COA and GA are used to obtain the parameters of the PV array model using the PV cell's datasheet information. The adopted models - using GA and COA - are implemented on a simulation platforms using MATLAB 2020a environment for two-diode and single-diode models. The proposed optimization method fits the mathematical current-voltage (I-V) characteristic to the three (V, I) remarkable points without the need to guess or to estimate any other parameter. The obtained models are tested and validated with experimental data taken from the Mutah university's PV power plant. The results show that for both of the employed optimization algorithms, the two-diode model is more accurate than the single-diode model. The results also disclose that, at different values of temperature and solar irradiance, the COA - compared to the GA - better handles the optimization problem with low iterations and better fitness value.

Keywords – Photovoltaic array; Photovoltaic cell; Genetic algorithm; Cuckoo optimization algorithm; Two-diode model; Single-diode model; Current-voltage characteristic.

1. INTRODUCTION

A photovoltaic (PV) system converts sunlight energy into electrical energy. The basic element of a PV system is the PV cell. Cells can be connected in series and/or parallel to form modules or panels and then large PV arrays. The term array is, usually, employed to describe a PV panel with several cells connected in series to obtain a certain operating voltage and/or in parallel to get higher current.

Modeling of PV arrays is widely introduced in the literature. The solution to the model's equations may be achieved by either analytical analysis or soft computing algorithms [1]. Whatever the approach is used, the two-diode model is more complex than other models of PV arrays. For this reason, limited research works have adopted this model [2-5]. In [2], the values of diode's currents I_{o1} and I_{o2} are assumed to be equal. This assumption makes the model less accurate since the I_{o2} is at least two orders of magnitude greater than I_{o1} [6]. In [3], researchers assume that the summation of the ideality factors is equal to a specific value where practically they are different. This assumption decreases the accuracy of the model. Other research works introduced new parameters to solve the two-diode model [5, 7, 8]. These techniques decrease the model accuracy due to the matching between the new parameters and the circuitry parameters.

In this work, the mathematical analysis of the adopted model is presented in detail. It forms an accurate current-voltage (I-V) model using intelligent techniques for obtaining the parameters of the two-diode model equation. This work aims to provide the researchers with all necessary information to develop PV array models and circuits that can be used in the

* Corresponding author

simulation of power converters for PV applications in a more accurate manner. A new parameter that measures the effect of temperature on diode's saturation current considering energy gap heat effect is introduced. In addition, two optimization algorithms are used to solve the model optimization problem, namely the cuckoo optimization algorithm (COA) and the genetic algorithm (GA) where their optimization processes are based on the sum squared error between a measured open-circuit voltage and the calculated - using the adopted optimized model - open-circuit voltage. A comparison between the results of both algorithms is presented using single and two diode models.

The rest of the paper is organized as follows: section 2 presents the effect of the non-ideal parameters on the two-diode model. The mathematical derivation of the cost function and the constraints are presented in section 3. The simulation results of the two presented algorithms are presented in section 4. The model validation and conclusions are presented in sections 5 and 6, respectively.

2. MODELS OF THE PV ARRAYS

In this section, the basic relations for ideal PV cell and two-diode model of the PV cell are presented and the effect of non-ideal parameters on the cell's I-V characteristic is covered.

2.1. Ideal Model

The equivalent circuit of the ideal PV cell is shown in Fig. 1. The basic equation that mathematically describes the output I-V characteristic of the ideal PV cell is given by [9, 10]:

$$I = I_{ph} - I_{o1} \left(e^{\frac{qV}{AK_bT}} - 1 \right) \quad (1)$$

where I_{ph} is the photoelectric current, I_{o1} is diode saturation current, K_b is Boltzmann constant, T is temperature in Kelvin, q is the electron charge, A is diode ideality factor.

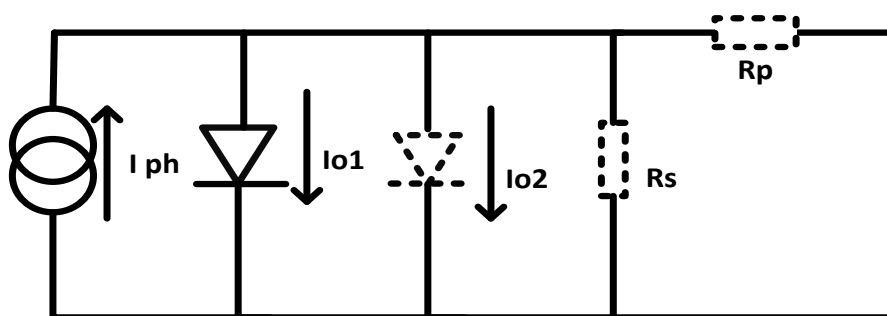


Fig. 1. Equivalent circuits of an ideal (full line) and a non-ideal (dotted line) solar cell.

It is well known that electric generators can be classified as current or voltage sources. The practical PV cell presents a hybrid behavior; i.e., it may act as a current source or voltage source depending on its operating point as shown in Fig. 2 [11].

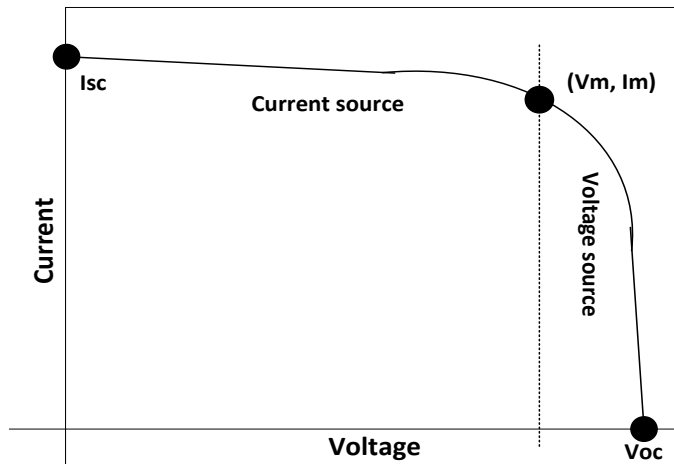


Fig. 2. I-V characteristic of a practical PV cell.

2.2. Non-Ideal Model

In the two-diode model, three non-ideal components can be added to the ideal model to achieve high accuracy. This model is used in this paper because it is more accurate than the single diode model [12-15]. In [16], a three-diode model is proposed to include the influence of components that are not considered by the two diode model. The single diode model was used by several authors, sometimes with simplifications but always with the basic structure composed of a current source and a parallel diode [17-28]. From Fig. 1, the non-ideal I-V equation can be written as:

$$I = I_{ph} - I_{o1} \left(e^{\frac{qV_d}{A_1 K_b T}} - 1 \right) - I_{o2} \left(e^{\frac{qV_d}{A_2 K_b T}} - 1 \right) - \frac{V + I R_s}{R_p} \quad (2)$$

where R_s and R_p are the series and parallel resistances, respectively. The second diode increases the accuracy of the maximum power point of the diode. The slope of the curve on its current source and voltage source regions depends on the value of the shunt and series resistances, respectively. Therefore, the ideal PV cell has zero slope in the current source region (pure current source) and infinite slope at the voltage source region (ideal voltage source). Figs. 3 and 4 show the effect of the series and shunt resistances and the second diode on the ideal I-V characteristic, respectively [10].

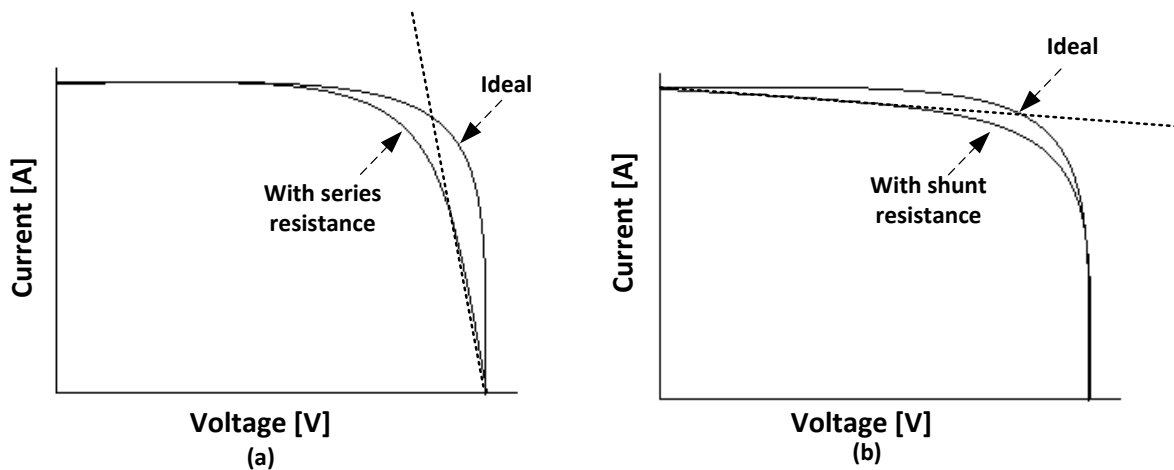


Fig. 3. Effect of the a) series resistance; b) shunt resistance on the ideal I-V characteristic.

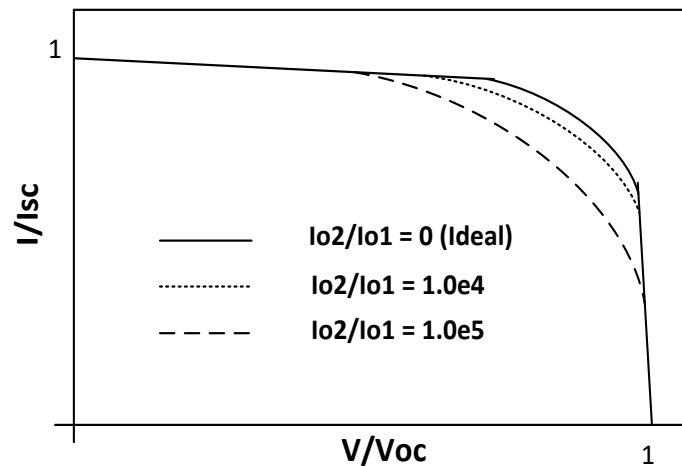


Fig. 4. Effect of the second diode on the ideal characteristic.

3. THE PROPOSED MODEL

3.1. Model Identification

At any operating point of the two-diode model, the output current (I) can be found as follow:

$$I_{ph} = I_{d1} + I_{d2} + I_p + I \quad (3)$$

where I_{d1} and I_{d2} are the diodes currents and I_p is the shunt resistor current. They may be written as follow:

$$I_{d1} = I_{o1} \left(e^{\frac{V+IR_s}{A_1 K T} q} - 1 \right) \quad (3a)$$

$$I_{d2} = I_{o2} \left(e^{\frac{V+IR_s}{A_2 K T} q} - 1 \right) \quad (3b)$$

$$I_p = \frac{V + I R_s}{R_p} \quad (3c)$$

where A_1 , A_2 are the ideality factors of diodes 1 and 2, respectively, I_{o2} is diode 2 saturation current, K is the Boltzmann constant T is the absolute temperature in Kelvin. The proposed model uses a single PV cell in its equation instead of the PV module, so the conversion between PV cell's model and the PVmodule's model can be written - based on the number of series-connected cells (N_s) and parallel-connected cells (N_p) - as follows:

$$V_{pv\ model} = N_s * V_{pv\ cell} \quad (4a)$$

$$I_{pv\ model} = N_p * I_{pv\ cell} \quad (4b)$$

$$R_{s\ moule} = \frac{N_s}{N_p} R_{s\ cell} \quad (4c)$$

$$R_{p\ moule} = \frac{N_p}{N_s} R_{p\ cell} \quad (4d)$$

Each of photoelectric current and diode current is sensitive to temperature as well as to solar irradiance. From the short circuit condition the I_{ph} can be driven as follow:

$$I_{ph} = I_{sc}(1 + \alpha\Delta T) \frac{G}{G_r} \left(1 + \frac{R_s}{R_p}\right) \quad (5)$$

where, I_{sc} , α , G , G_r are the short circuit current, temperature coefficient on short circuit current, solar irradiance, and solar irradiance under standard condition, respectively. The diode saturation current is the most important part of this model because of its high sensitivity to temperature variation. The most common saturation current model is [29-35]:

$$I_o = I_{or} \left(\frac{T}{T_r}\right)^{\frac{3}{A}} \cdot \exp\left\{\frac{E q}{A K} \left(\frac{1}{T_r} - \frac{1}{T}\right)\right\} \quad (6a)$$

where I_{or} is the diode's saturation current at reference temperature (T_r) and E is the energy gap which depends on the temperature as follow:

$$E = E_0 - \frac{\alpha T^2}{\beta + T} \quad (6b)$$

where, $E_0 = 1.17 \text{ eV}$, $\alpha = 4.73 \times 10^{-4} \frac{\text{eV}}{\text{K}^2}$, $\beta = 636\text{K}$ for Silicon. As a result, the saturation current can be written as:

$$I_o = I_{or} \left(\frac{T}{T_r}\right)^{\frac{3}{A}} \exp\left(\frac{H}{A}\right) \quad (6c)$$

where H is the heat effect factor given by:

$$H = \frac{T^3 + a_1 T^2 + a_2 T + a_3}{T^2 + b T} C$$

where a_1 , a_2 , a_3 , b and C are constants that do not depend on the temperature and given by:

$$a_1 = -\left(\frac{E_0}{\alpha} + T_r\right),$$

$$a_2 = -\frac{E_0}{\alpha} (\beta - T_r),$$

$$a_3 = \frac{E_0}{\alpha} \beta T_r,$$

$$b = \beta, \quad C = \frac{-\alpha q}{T_r k}$$

The diode's current can be written as follow:

$$I_{d1} = I_{or1} \left(\frac{T}{T_r}\right)^{\frac{3}{A_1}} \exp\left(\frac{H}{A_1}\right) \left(\exp\left(\frac{V + IR_s}{A_1 K T} q\right) - 1\right) \quad (7a)$$

$$I_{d2} = I_{or2} \left(\frac{T}{T_r}\right)^{\frac{3}{A_2}} \exp\left(\frac{H}{A_2}\right) \left(\exp\left(\frac{V + IR_s}{A_2 K T} q\right) - 1\right) \quad (7b)$$

3.2. Problem Definition, Fitness Function, and Constraints

Three constraints are defined for the optimization problem as follow:

- Open circuit constraint: $V = V_{oc}$, $I = 0$.

- Maximum power point constraint: $V = V_m, I = I_m$.
- Maximum power slope constraint: $\frac{\partial P}{\partial V}(V_m, I_m) = 0$.

The cost function (E) is defined as follow:

$$E = \sum_{T=0^{\circ}\text{C}}^{T=70^{\circ}\text{C}} \left| \frac{V_{oc-m} - V_{oc-c}}{V_{oc-m}} \right| * 100 \% \quad (8)$$

where V_{oc-c} is the calculated open-circuit voltage and V_{oc-m} is the measured open-circuit voltage.

To find the calculated open-circuit voltage V_{oc-c} at temperature T, the following relation is used :

$$I_{sc}(1 + \alpha\Delta T) \frac{G}{G_r} \left(1 + \frac{R_s}{R_p}\right) = I_{o1} \exp \left\{ \frac{V_{oc}}{A_1 k T} q \right\} + I_{o2} \exp \left\{ \frac{V_{oc}}{A_2 k T} q \right\} + \frac{V_{oc}}{R_p} \quad (9a)$$

The measured open-circuit voltage V_{oc-m} is given as:

$$V_{oc-m} = V_{ocr}(1 + \beta\Delta T) \quad (9b)$$

The optimization problem - based on previous model equations - solves the constant parameters ($I_{or1}, I_{or2}, A_1, A_2, R_s, R_p$) based on the reference values of the parameters ($V_{oc}, I_{sc}, V_m, I_m, \alpha, \beta, N_{cell}$) presented in the PV model's datasheet.

3.3. Boundary Limitations

The minimum value of R_p which is the slope of the line segment between the short-circuit point and the maximum power point is given by:

$$R_p \min = \frac{V_m}{I_{sc} - I_m} \quad (10a)$$

Similarly, the maximum value of R_s which is the slope of the line segment between the open-circuit and the maximum power point is presented as:

$$R_s \max = \frac{V_{oc} - V_m}{I_m} \quad (10b)$$

4. SIMULATION RESULTS

The parameters of the JAM6(K)-72-340/PR PV module (which is used in the Mutah university PV-power plant) are adopted to validate the proposed model. Table 1 shows the datasheet of JAM6(K)-72-340/PR PV module. Data is measured at standard test condition (STC) where each array contains 72 series-connected cells, with 340 W maximum power. For the aim of finding the cell's parameters from the array parameter, Eq. (4) is used.

Table 1. Parameters of the JAM6 (K)-72-340/PR PV module at 25 °C and G = 1000 W/m².

V_m (V)	I_m (A)	V_{oc} (V)	I_{sc} (A)	α (%/C°)	β (%/C°)	N_s	N_p
38.18	8.91	46.86	9.46	0.06	-0.3	72	1

To solve the optimization problem using GA and a COA for both single and two diode models, MATLAB 2020a is used. The utilized GA optimizes the PV model's parameters. The GA population size affects both the GA performance and efficiency. Generally, GA performs poorly if a very small population is used; this is because an insufficient sample size is not

provided [36]. In contrast, large populations require more evaluations per generation which can result in an unacceptable demand for processing and a slow rate of convergence. Here, in our simulation, the population size is chosen to be 30 based on results of the error analysis conducted in this work. Besides, for the adopted application, the best value for the crossover rate was found to be equal to 0.67. This value is chosen according to some trial simulations conducted for this purpose. Consequently, the mutation rate is chosen to be 0.005, according to previous studies conducted by some researchers. In the simulations presented in this work, 8-bit chromosomes are used for each variable of optimized and linear scaling fitness technique where the better strings reproduce more copies in the next generation.

The COA is very sensitive to its parameters; i.e., the setting of the parameters can affect its efficiency [37]. The parameter settings cause more reliability and flexibility of the algorithm. So, settings the parameters are one of the crucial factors to gain an optimized solution in all optimization problems. Table 2 shows the selected parameters for the proposed COA.

Table 2. Parameters settings of COA.

Parameter	Value
Number of cuckoos	100
Minimum number of eggs	2
Maximum number of eggs	4
Maximum iteration	123
Number of clusters	2
Lower band of parameter	0.1
Higher band of parameter	1000
Maximum number of cuckoos	10
Radius coefficient	5

To investigate the performance of the GA and COA for PV modeling, the fitness cost function presented in Eq. (8) which maps the cost function value to the fitness value is adopted. Here, the optimization problem is solved for finding the constant parameters (I_{or1} , I_{or2} , A_1 , A_2 , R_s , R_p) of the model in which they are related to the reference parameters (v_{oc} , I_{sc} , V_m , I_m , α , β , N_{cell}) presented in the datasheet. In the case of the single diode model used, both I_{or2} and A_2 are removed.

4.1. Single Diode Model

In the single-diode model, the optimization algorithms are used to set four parameters (I_{or} , A , R_s , R_p) rather than six. The convergence results are depicted in Figs. 5 and 6 for GA and COA, respectively. Besides, the obtained four optimized parameters are shown in Figs. 7 and 8 for both algorithms.

Figs. 9 and 10 show the I-V and power characteristics at different temperatures and solar irradiances for the COA. Figs. 11 and 12 show the 3-D I-V and power characteristics for the GA.

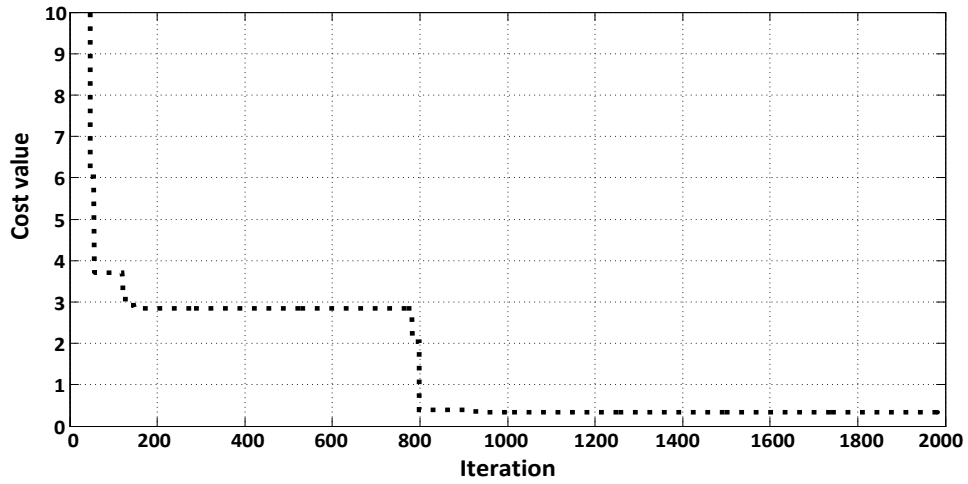


Fig. 5. Fitness function using GA for the single-diode model.

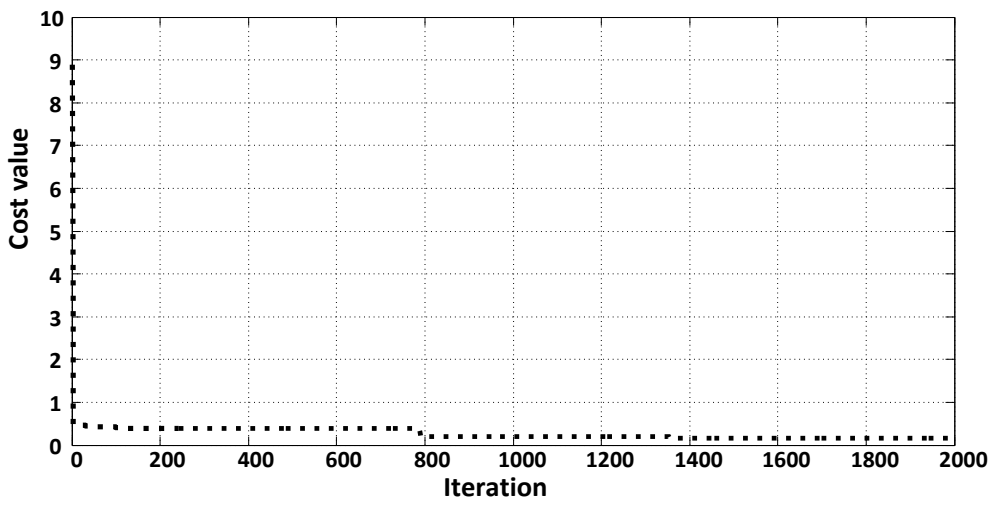


Fig. 6. Fitness function using the COA for the single-diode model.

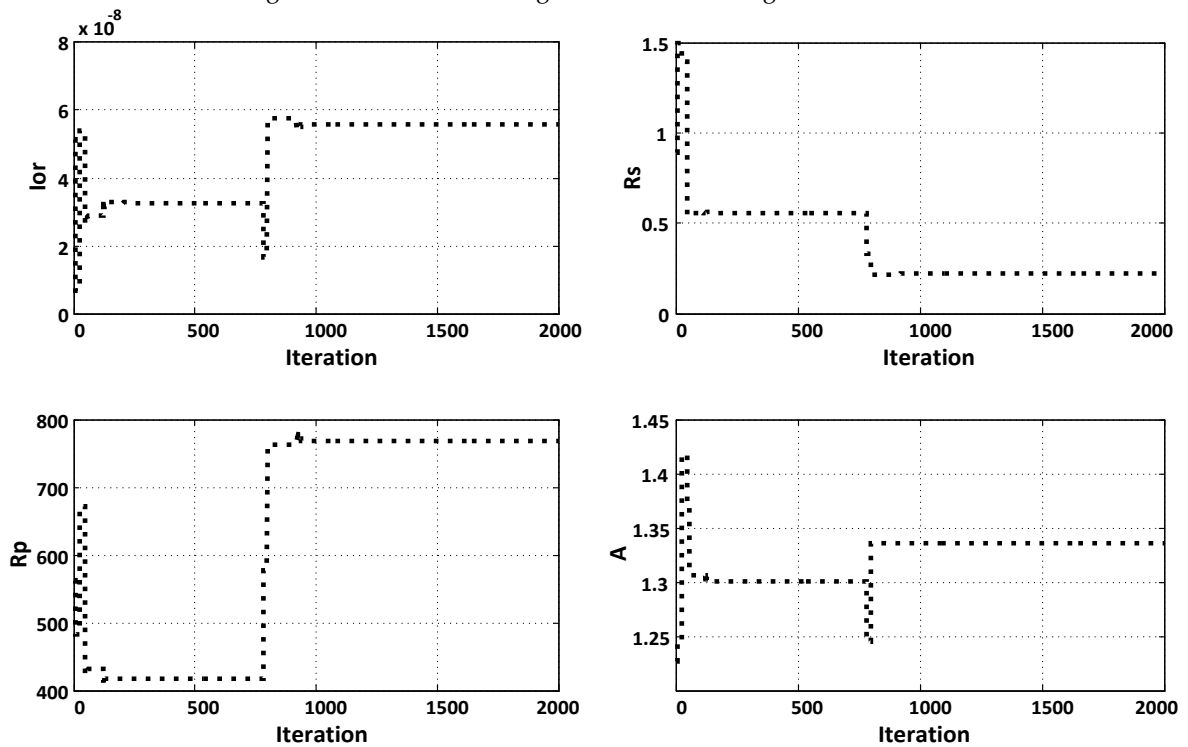


Fig. 7. Optimized parameters using the GA algorithm for the single-diode model.

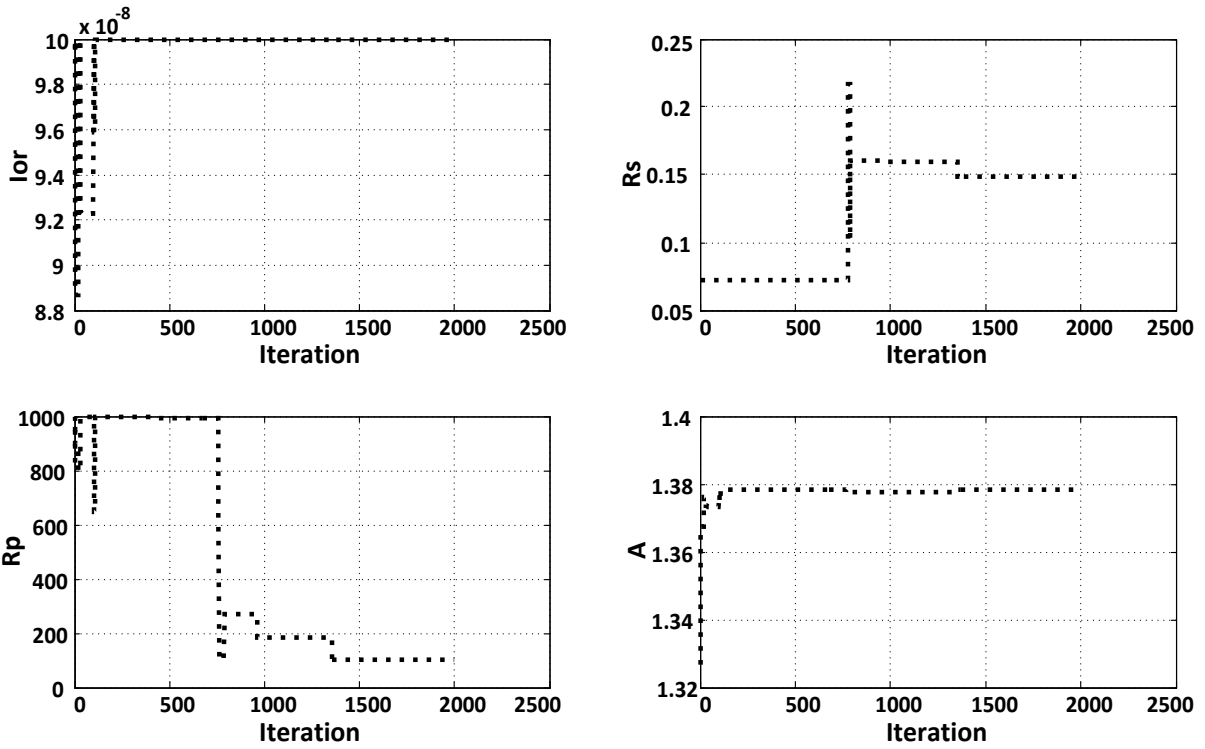


Fig. 8. Optimized parameters using the COA for the single-diode model.

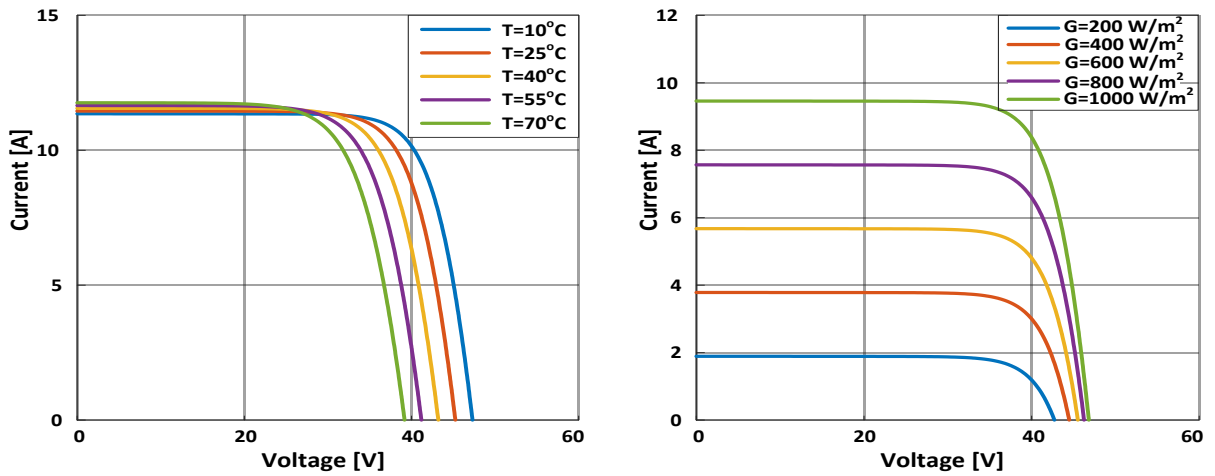


Fig. 9. I-V characteristics using the COA for the single-diode model.

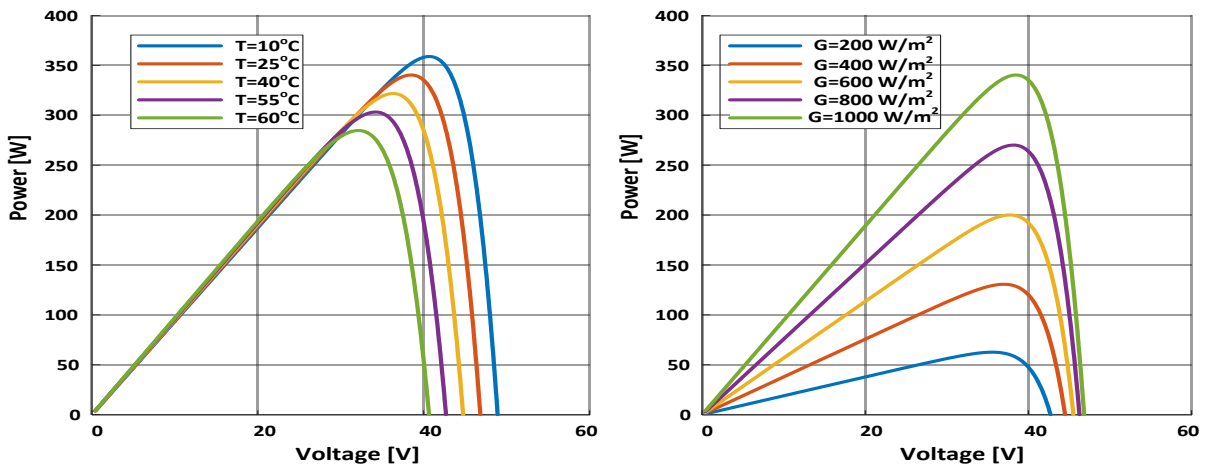


Fig. 10. Power characteristics using the COA for the single-diode model.

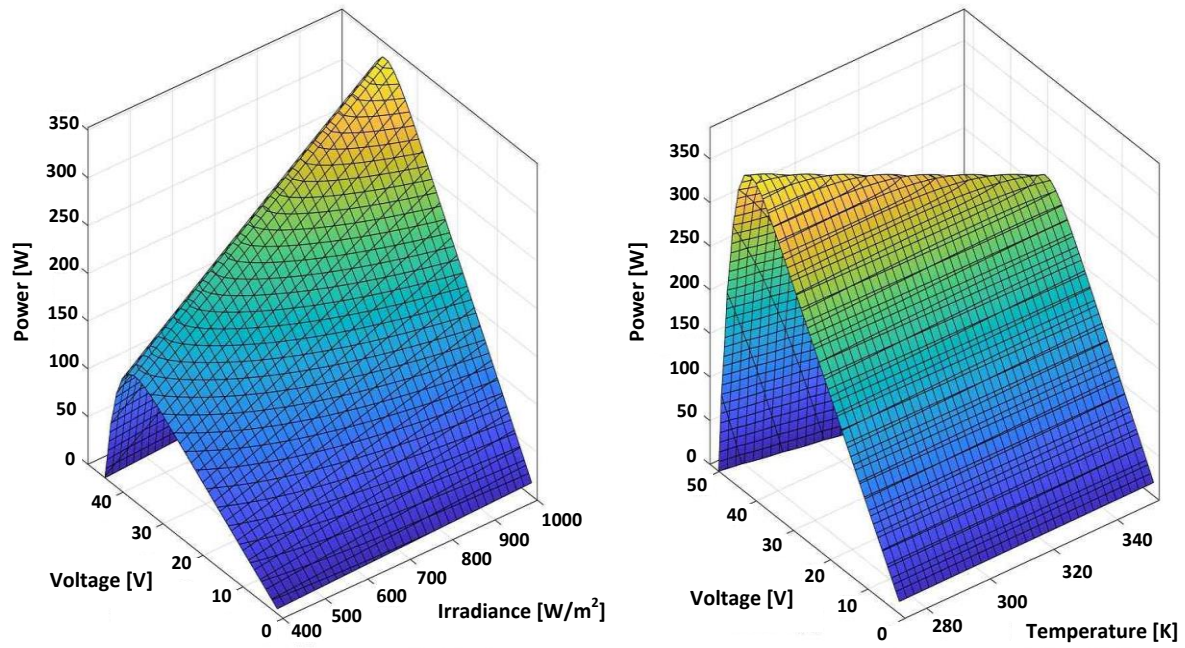


Fig. 11. 3-D I-V characteristics using the GA for the single-diode model.

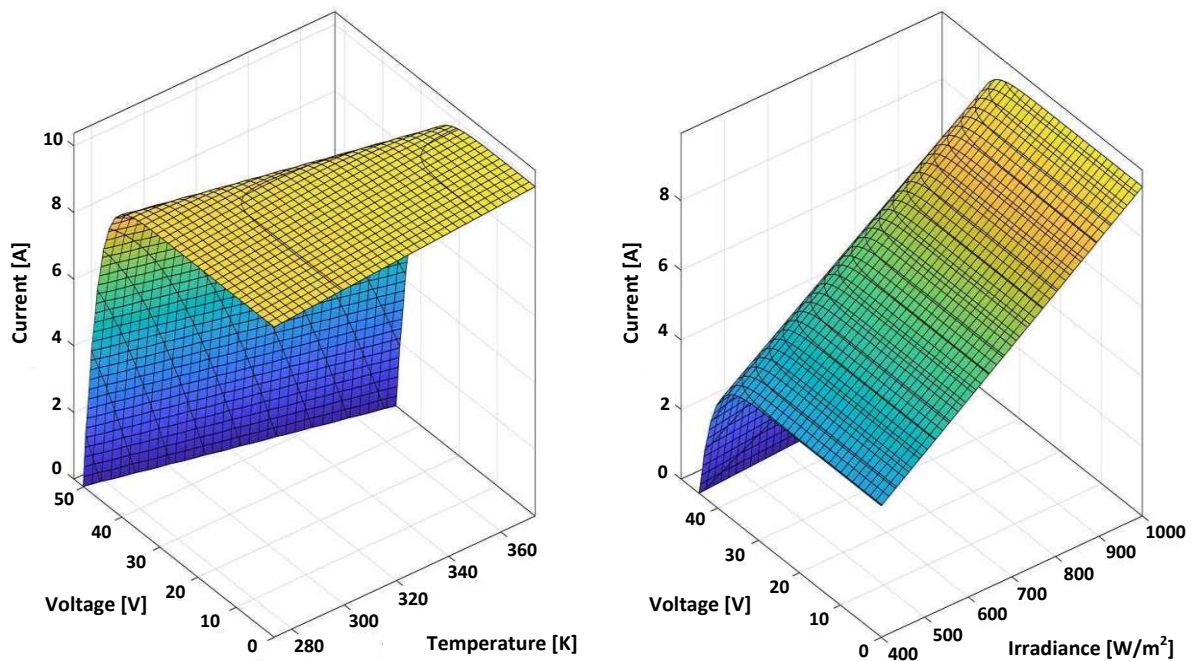


Fig. 12. 3-D power characteristics using the GA for the single-diode model.

4.2. Two-Diode Model

Figs. 13-16 show the fitness function of the two-diode model, and the optimized parameters using the adopted GA and COA. Besides, the I-V and the power characteristics with the variation of temperature and irradiance levels obtained using the GA and COA are illustrated in Figs. 17-20.

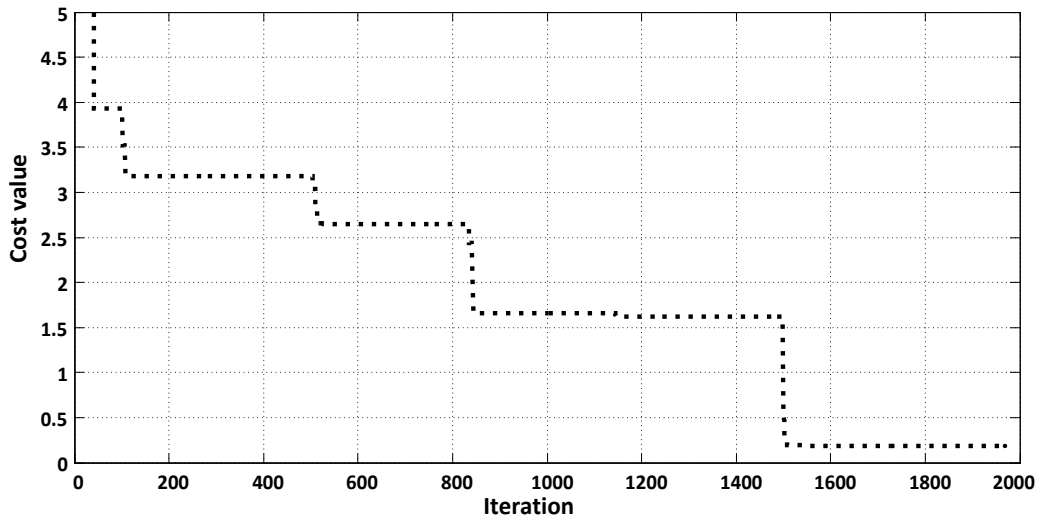


Fig. 13. Fitness function using the GA for the two-diode model.

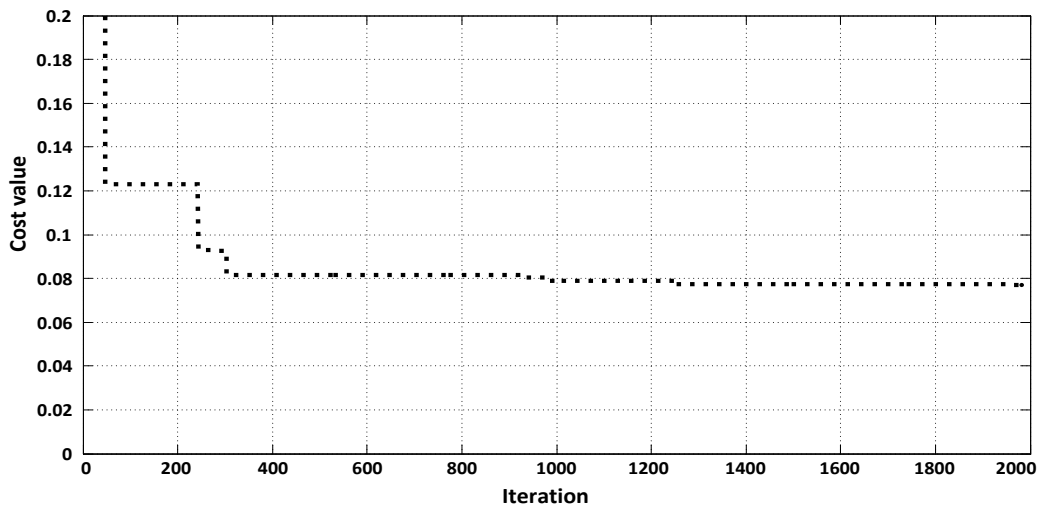


Fig. 14. Fitness function using the COA for the two-diode model.

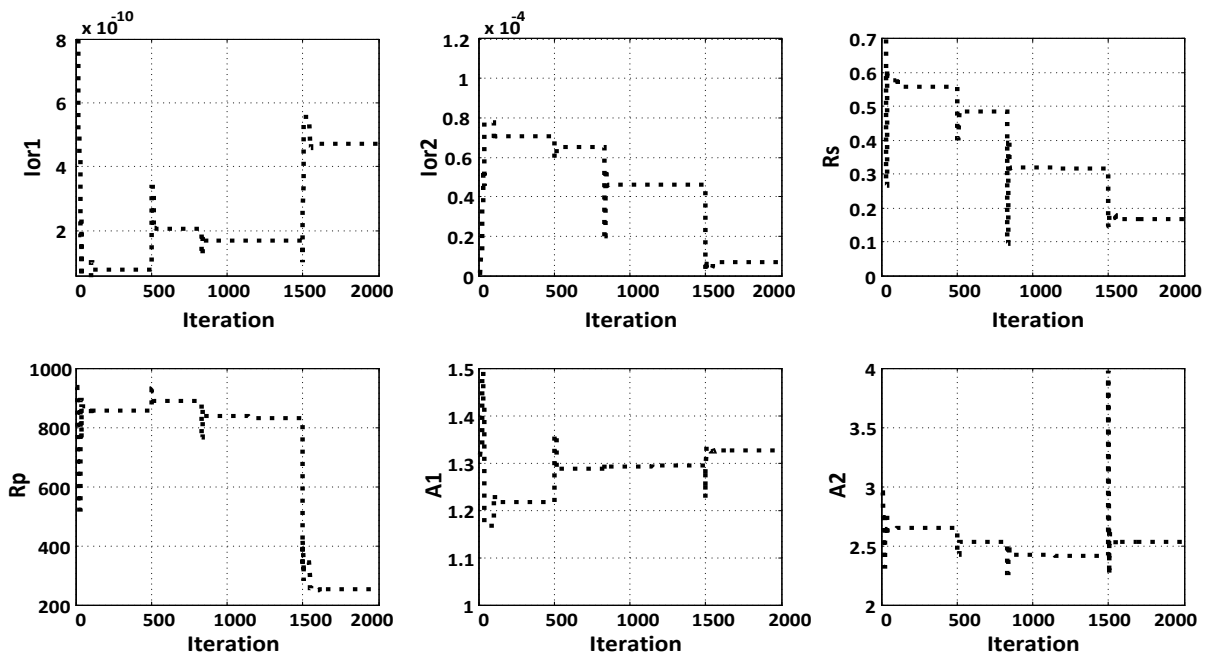


Fig. 15. Optimized parameters using the GA for the two-diode model.

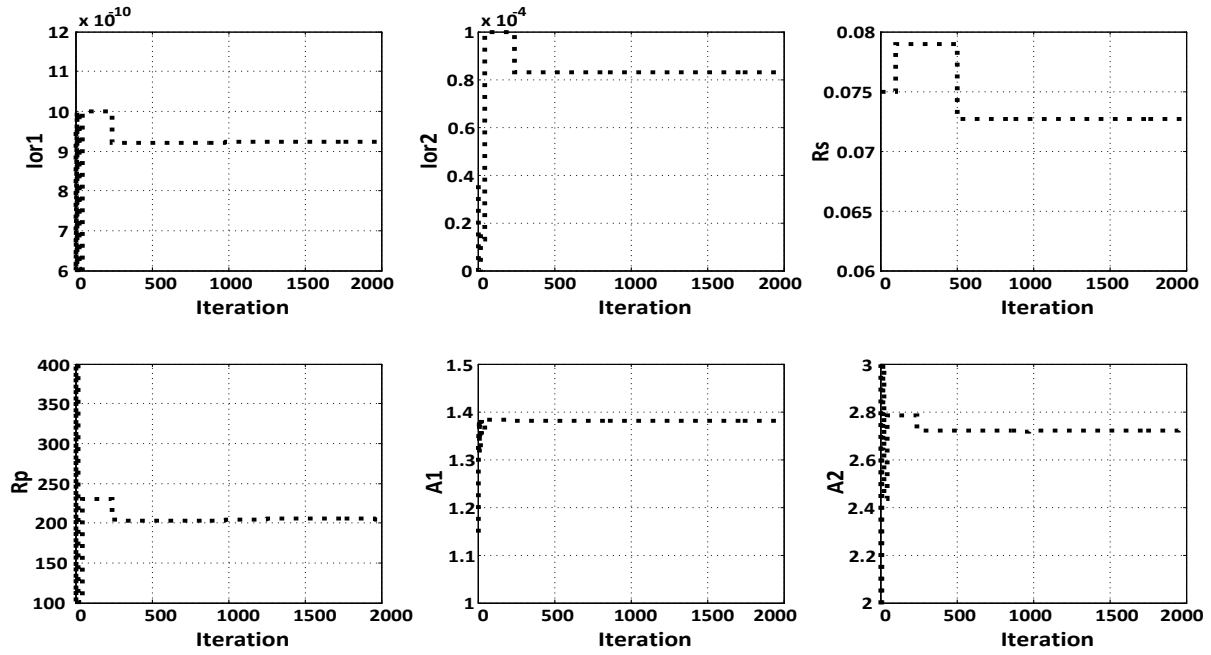


Fig. 16. Optimized parameters using the COA for the two-diode model.

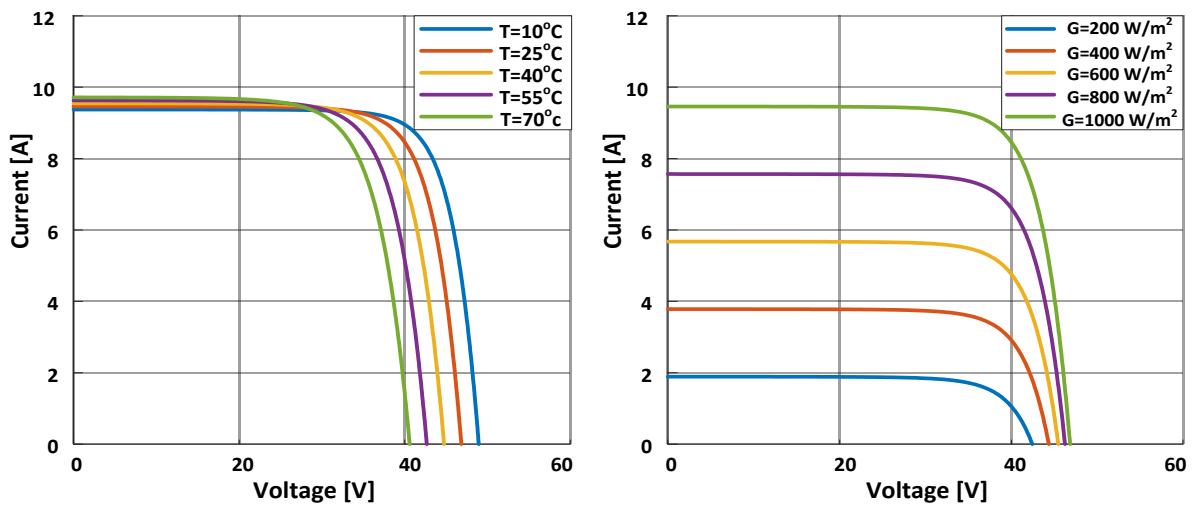


Fig. 17. I-V characteristics using the COA for the two-diode model.

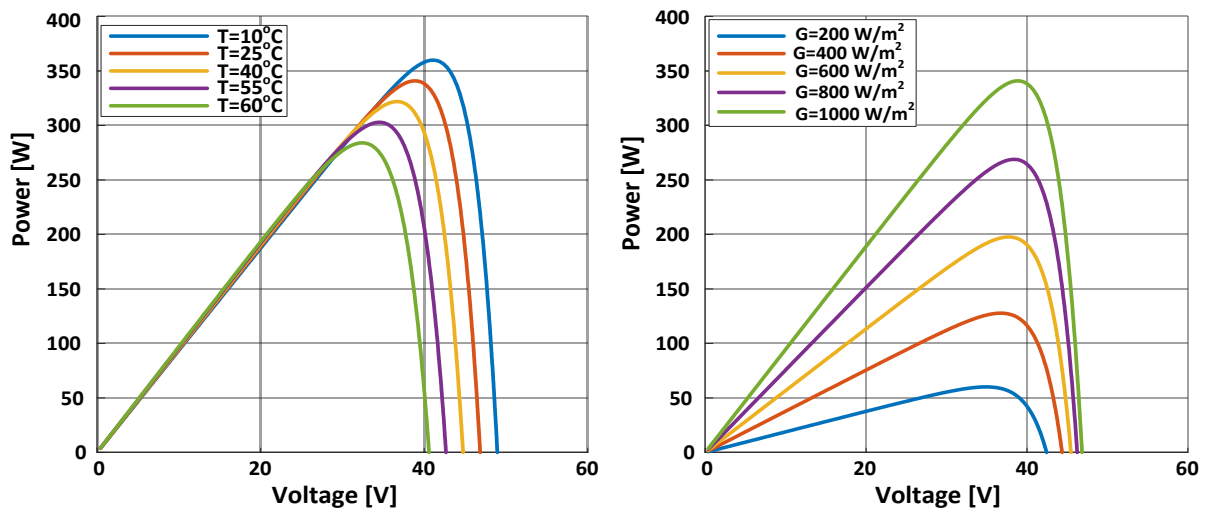


Fig. 18. Power characteristics using the COA for the two-diode model.

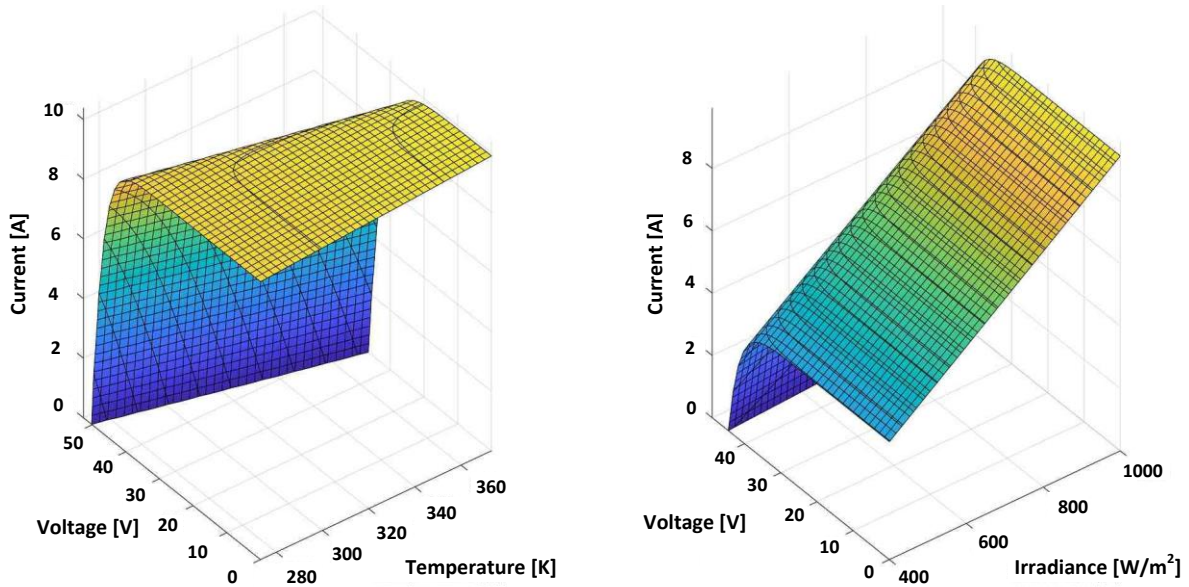


Fig. 19. 3-D I-V characteristics using the GA algorithm for the two-diode model.

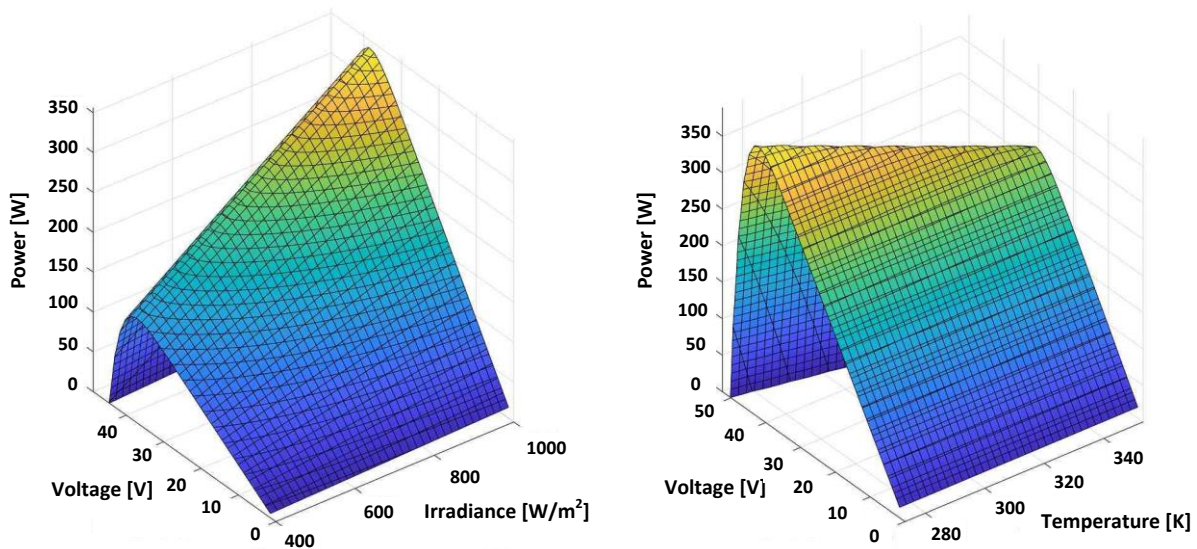


Fig. 20. 3-D power characteristic using the GA for the two-diode model.

4.3. Analysis of the Obtained Results

In this work, the number of nests was set to 25 for the COA since any number between 15 and 40 is sufficient for most optimization problems while the total of iterations was 200. Due to the stochastic nature of the COA, the start points for the algorithm are not the same and the paths followed are also different. To address these differences, each optimization algorithm was run many times and the most efficient results, obtained with minimum error - as compared with reference values - are the ones considered for this work. Table 3 summarizes the results of the previous two subsections. Based on the them, it is observed that the two-diode model is more accurate than the single diode model. The fitness value in the case of the used GA is decreased from 0.3433 % to 0.18937 % when using the two diode model rather than one diode model, where the ratio $\frac{I_{or2}}{I_{or1}}$ is about 140. Similarly, the results of the two-diode model in the the case of COA is more accurate than those of the one diode model. The error is decreased from 0.17 % to 0.07 % where the saturation currents ratio is about 800. Both models'

I-V characteristics are plotted together at standard test conditions in Fig. 21. The difference between one diode model's series resistance and two diode model's series resistance is seen at the slope of the curve at the open-circuit voltage point.

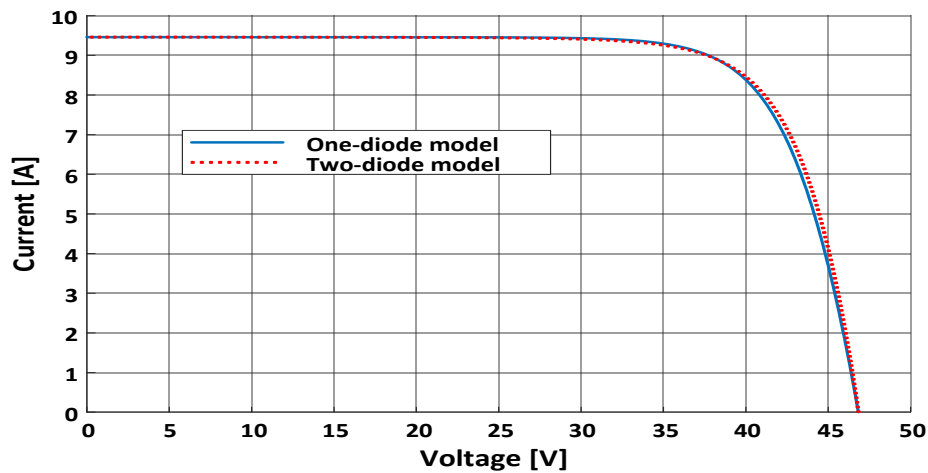


Fig. 21. I-V characteristics using the COA for the investigated diode models.

The obtained results show that the the COA gives a better solution than GA. In both models, the COA algorithm is more appropriate than GA to handle the optimization problem. From table 3, it can be seen that the fitness value in the COA is less than the half-value obtained by GA. On the other hand, at the same number of iterations, the COA takes more computational time than GA.

From the characteristics of the PV cell, the module is directly dependent on the irradiation and the temperature. Current and power - as a function of the voltage for different levels of irradiation at a constant temperature of 25 °C - change considerably, while the voltage changes slightly with the irradiation. On the other hand - current and power - as a function of the voltage for different temperature levels with a constant irradiation level of constant 1000 W/m², show a slight change, while the voltage changes slightly with temperature.

Table 3. Optimized parameters for both diode models using GA and COA.

Algorithm variable	Single-diode model		Two-diode model	
	GA	COA	GA	COA
I_{or1}	5.5748e-8	1e-7	4.7201 e-08	9.2409e-8
I_{or2}	-	-	6.6864e-6	8.3157e-5
A_1	1.3355	1.3785	1.3257	1.3799
A_2	-	-	2.4225	2.727
R_s	0.21938	0.15264	0.16764	0.0727
R_p	767.9718	100	251.3	204.9
Fitness value	0.3433 %	0.17 %	0.18937 %	0.077108%
Number of iteration	2000	2000	2000	2000
Simulation time [s]	197.5	365.7	132	152.0

5. MODEL TEST VALIDATION

In this section, validation of the proposed model is presented using the results of the model's optimized parameters obtained using the COA. Two validation methods are applied, namely curve fitting and actual validation using data from Mutah university solar power plant. The first method uses I-V and power characteristics from the datasheet and plots model characteristics at different levels of temperatures and solar irradiance. In this method, all possible operating points are validated at different levels of temperature and solar irradiance.

Figs. 22-24 show a comparison between the I-V and power characteristic obtained from the datasheet with those of the proposed model at different diffent levels of temperatures and solar irradiance. On these figures, solid lines refer to data-sheet curves and dashed-lines refer to model curves. In these curves, the two-diode model with COA is used to compare the results with 345W mono 72 Cells from the same family of the previous module.

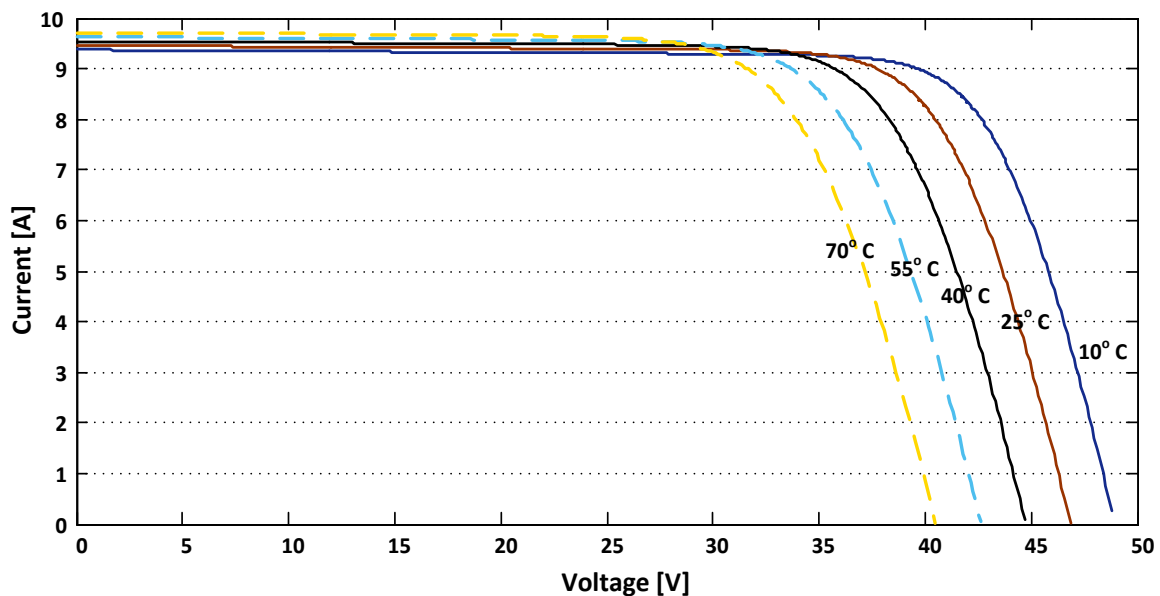


Fig. 22. I-V characteristics at different temperatures values and at an irradiance level of 1000 W/m^2 .

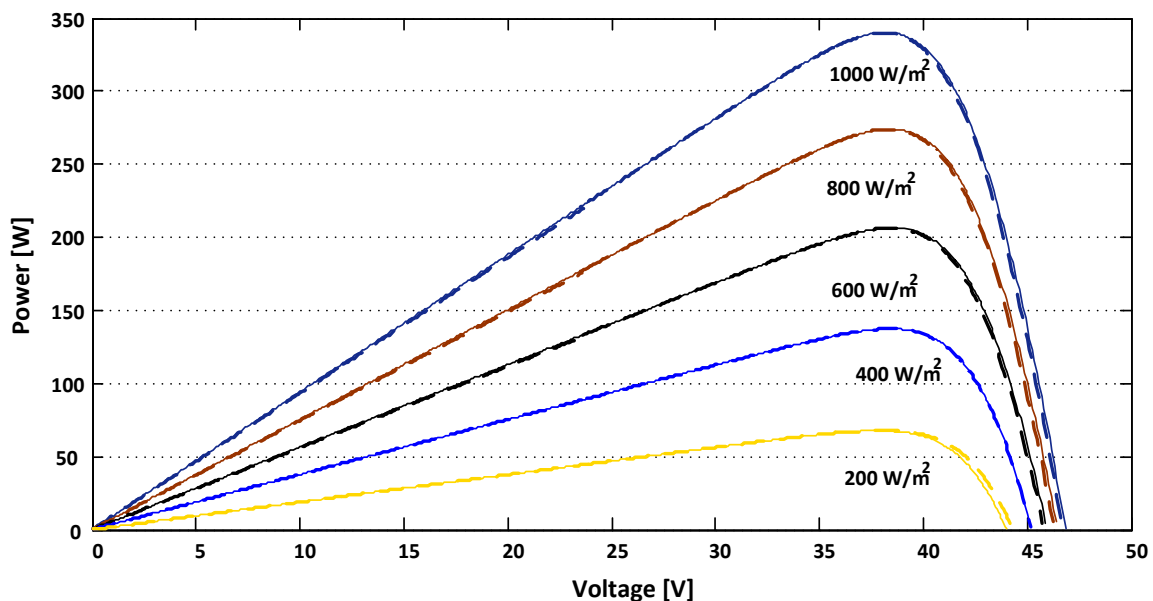


Fig. 23. Power characteristics at different irradiance levels at a temperature of 25°C .

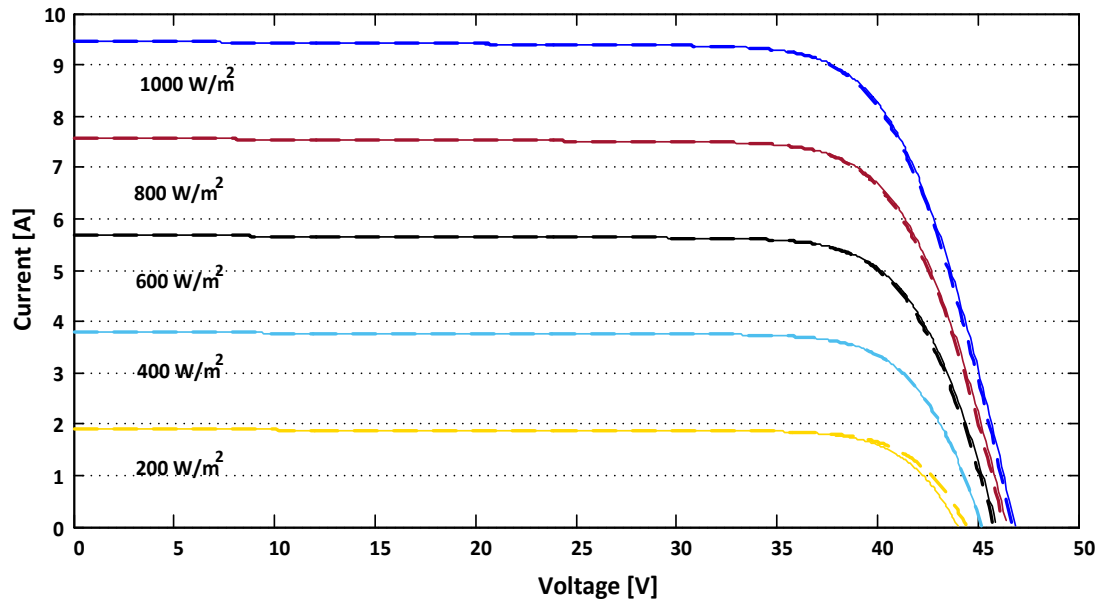


Fig. 24. I-V characteristics at different irradiance levels with $T = 25^{\circ}\text{C}$.

The second validation method compares the result with actual measured points from the 5 MW Mutah university PV-plant that contains 4, 1.5 MVA medium voltage transformers, with 84 inverters. Each inverter is connected to a combiner box with input from 10 parallel strings of 18 series arrays in each string.

Table 4 shows some examples of operations taken at different times. In table 4, the absolute error in current is calculated based on the difference between the actual measured current (I_m) and the calculated current by the proposed model (I_c).

The temperature of the array (T) and solar irradiance (S) are measured individually at each time. Voltage (V) and current (I_m) are measured at the inverter's DC-input side; the voltage drop on the DC-cable (from the combiner box to inverter) is considered. Drop voltage on wires which connect arrays to the combiner box is ignored because the combiner is installed on the back of each group of strings. The model is modified to an appropriate inverter group in the same way used in Eq. (4). The simulation model of the proposed PV using MATLAB Simulink is shown in Figs. 25 and 26.

Table 4. Results of the second validation method (actual validation).

T [C]	G [w/m ²]	V [V]	I_m [A]	I_c [A]	E [%]
43.8	1012	667.1	80.22	80.8	0.73
51.6	994	656.9	75.63	76.43	1.06
54.3	991	659.5	70.39	71.03	0.091
55.3	997	656.8	70.17	70.97	1.14
51.6	996	660.2	74.73	75.48	1.00
51.8	1005	657.2	75.54	76.67	0.736
56.2	971	648.00	71.61	72.32	0.99

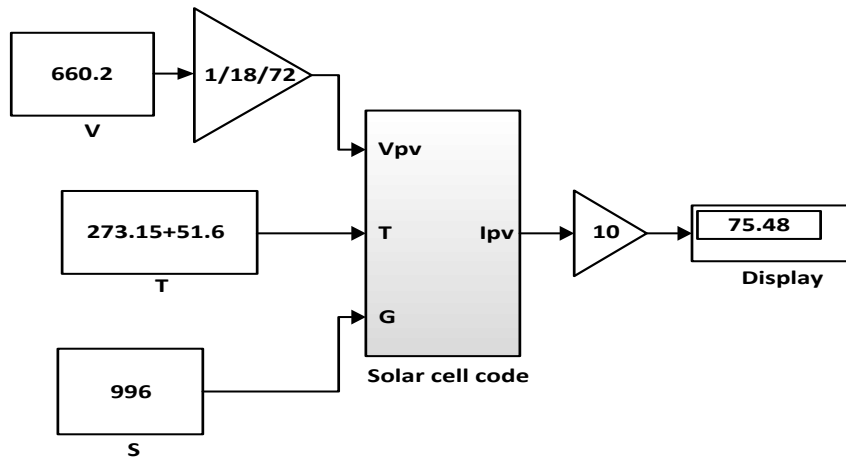


Fig. 25. Simulink’s simulation model using the COA of the two-diode model.

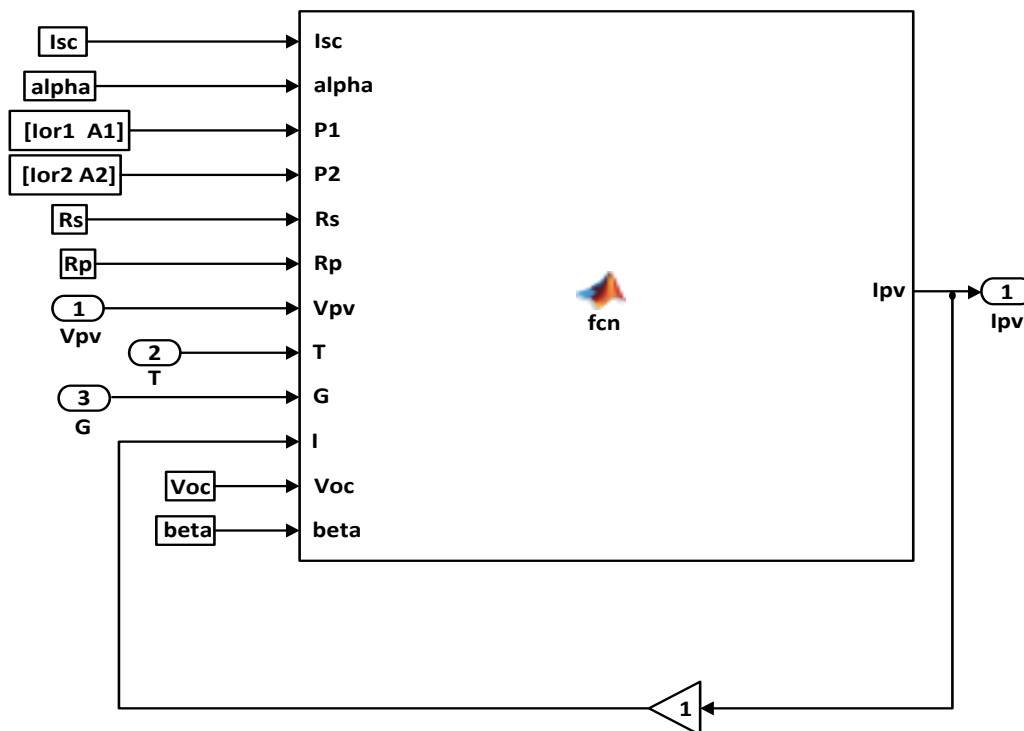


Fig. 26. Simulink’s simulation model of the PV cell.

6. CONCLUSIONS

This paper proposed an indirect method - based on artificial intelligent techniques (GA and COA) - to adjust the mathematical I-V characteristic of a PV array. The objective of the method is to fit the mathematical I-V equation to the experimental remarkable points of the practical PV array and the datasheet I-V curve. The method obtained the proposed new parameters of the I-V equation using the following nominal parameters from the PV array’s datasheet: open-circuit voltage, short-circuit current, maximum output power, voltage, and current at the maximum power point, current/temperature, and voltage/temperature coefficients. The proposed optimization method fitted the mathematical I-V curve to the three (V, I) remarkable points without the need to guess or to estimate any other parameter. The two-diode model was used to modeling the PV module and the single-diode model is used for comparison.

The obtained result showed that at different temperatures and solar irradiances, the COA could solve the defined optimization problem better than GA. The accuracy of the solution using COA is better than a genetic algorithm with a lower number of iterations. However, the computational time of the COA is larger than the GA. The results also revealed that for both of the employed optimization algorithms, the two diode model showed to be more accurate than the one diode model.

REFERENCES

- [1] V. Chin, Z. Salam, K. Ishaque, "Cell modeling and model parameters estimation techniques for PV simulator application: a review," *Applied Energy*, vol. 154, pp. 500–519, 2015.
- [2] K. Ishaque, Z. Salam, H. Taheri, "Simple, fast and accurate two-diode model for PV modules," *Solar Energy Materials and Solar Cells*, vol. 95, no. 2, pp. 586–594, 2011.
- [3] A. Elbaset, H. Ali, M. Abd-El Sattar, "Novel seven-parameter model for PV modules," *Solar Energy Materials and Solar Cells*, vol. 130, pp. 442–455, 2014.
- [4] B. Babu, S. Gurjar, "A novel simplified two-diode model of PV (PV) module," *IEEE Journal of PVs*, vol. 4, no. 4, pp. 1156–1161, 2014.
- [5] M. Hijri, H. Mokhtari, M. Azizian, M. Ghandhari, L. Soder, "On the parameter extraction of a five-parameter double-diode model of PV cells and modules," *IEEE Journal of PVs*, vol. 4, no. 3, pp. 915–923, 2014.
- [6] M. Wolf, G. Noel, R. Stirn, "Investigation of the double exponential in the current-voltage characteristics of solar silicon cells," *IEEE Transactions on Electron Devices*, vol. 24, no. 4, pp. 419–428, 1977.
- [7] K. Ishaque, Z. Salam, S. Mekhilef, A. Shamsudin, "Parameter extraction of solar PV modules using penalty-based differential evolution," *Applied Energy*, vol. 99, pp. 297–308, 2012.
- [8] J. Gow, C. Manning, "Development of a PV array model for use in power-electronics simulation studies," *IEE Proceedings-Electric Power Applications*, vol. 146, no. 2, pp. 193–200, 1999.
- [9] H. Rauschenbach, *Solar Cell Array Design Handbook*, Van Nostrand Reinhold, 1980.
- [10] T. Markvart, A. McEvoy, L. Castafier, *Practical Handbook of PVs: Fundamentals and Applications*, Elsevier Science Inc., New York, 2003.
- [11] J. Gow, C. Manning, "Development of a model for PV arrays suitable for use in simulation studies of solar energy conversion systems," *Proceedings of 6th International Conference on Power Electronics and Variable Speed Drives*, pp. 69–74, 1996.
- [12] N. Pongratananukul, T. Kasparis, "Tool for automated simulation of solar arrays using general-purpose simulators," *Proceedings of IEEE Workshop on Computers in Power Electronics*, Urbana, IL, USA, pp. 10–14, 2004.
- [13] J. Gow, C. Manning, "Development of a PV array model for use in power-electronics simulation studies," *IEE Proceedings-Electric Power Applications*, vol. 146, no. 2, pp. 193–200, 1999.
- [14] S. Chowdhury, G. Taylor, S. Chowdhury, A. Saha, Y. Song, "Modeling, simulation and performance analysis of a PV array in an embedded environment," *Proceedings of 42nd International Universities Power Engineering Conference*, Brighton, pp. 781–785, 2007.
- [15] J. Hyvarinen, J. Karila, "New analysis method for crystalline silicon cells," *Proceedings of 3rd World Conference on PV Energy Conversion*, vol. 2, pp. 1521–1524, 2003.
- [16] K. Nishioka, N. Sakitani, Y. Uraoka, T. Fuyuki, "Analysis of multi-crystalline silicon solar cells by modified 3-diode equivalent circuit model taking leakage current through periphery into consideration," *Solar Energy Materials and Solar Cells*, vol. 91, no. 13, pp. 1222–1227, 2007.

- [17] A. Celik, N. Acikgoz, "Modelling and experimental verification of the operating current of monocrystalline PV modules using four- and five parameter models," *Applied Energy*, vol. 84, no. 1, pp. 1-15, 2007.
- [18] M. Veerachary, "PSIM circuit-oriented simulator model for the nonlinear PV sources," *IEEE Transactions on Aerospace and Electronic Systems*, vol. 42, no. 2, pp. 735-740, 2006.
- [19] Y. Kuo, T. Liang, J. Chen, "Novel maximum-power-point-tracking controller for PV energy conversion system," *IEEE Transactions on Industrial Electronics*, vol. 48, no. 3, pp. 594-601, 2001.
- [20] G. Ahmad, H. Hussein, H. El-Ghetany, "Theoretical analysis and experimental verification of PV modules," *Renewable Energy*, vol. 28, no. 8, pp. 1159-1168, 2003.
- [21] G. Walker, "Evaluating MPPT converter topologies using a MatLab PV model," *Journal of Electrical and Electronics Engineering*, vol. 21, no. 1, 2001.
- [22] E. Koutroulis, K. Kalaitzakis, V. Tzitzionis, "Development of an FPGA-based system for real-time simulation of PV modules," *Microelectronics Journal*, vol. 40, no. 7, pp. 1094-1102, 2009.
- [23] M. Vitorino, L. Hartmann, A. Lima, M. Correa, "Using the model of the solar cell for determining the maximum power point of PV systems," *Proceedings of European Conference on Power Electronics and Applications*, p. 1-10, 2007.
- [24] D. Sera, R. Teodorescu, P. Rodriguez, "PV panel model based on datasheet values," *Proceedings of IEEE International Symposium on Industrial Electronics*, pp. 2392-2396, 2007.
- [25] Y. Yusof, S. Sayuti, M. Abdul Latif, M. Wanik, "Modeling and simulation of maximum power point tracker for a PV system," *Proceedings of National Power and Energy Conference*, pp. 88-93, 2004.
- [26] W. Xiao, W. Dunford, A. Capel, "A novel modeling method for PV cells," *Proceedings of IEEE 35th Annual Power Electronics Specialists Conference*, Aachen, Germany, pp. 1950-1956, 2004.
- [27] S. Liu, R. Dougal, "Dynamic multiphysics model for a solar array," *IEEE Transactions on Energy Conversion*, vol. 17, no. 2, pp. 285-294, 2002.
- [28] M. Elhagry, A. Elkousy, M. Saleh, T. Elshatter, E. Abou-Elzahab, "Fuzzy modeling of PV panel equivalent circuit," *Proceedings of 40th Midwest Symposium on Circuits and Systems*, Sacramento, CA, USA, pp. 60-63, 1997.
- [29] M. Villalva, J. Gazoli, E. Filho, "Modeling and circuit-based simulation of PV arrays," *Brazilian Journal of Power Electronics*, vol. 14, no. 1, pp. 35-45, 2009.
- [30] W. De Soto, S. Klein, W. Beckman, "Improvement and validation of a model for PV array performance," *Solar Energy*, vol. 80, no. 1, pp. 78-88, 2006.
- [31] Q. Kou, S. Klein, W. Beckman, "A method for estimating the long-term performance of direct-coupled PV pumping systems," *Solar Energy*, vol. 64, no. 1-3, pp. 33-40, 1998.
- [32] R. A. Messenger and J. Ventre. "PV systems engineering," *CRC Press*, 2004.
- [33] F. Nakanishi, T. Ikegami, K. Ebihara, S. Kuriyama, Y. Shiota, "Modeling and operation of a 10 kW PV power generator using equivalent electric circuit method," *Conference Record of the 28th IEEE PV Specialists Conference*, Anchorage, AK, USA, pp. 1703-1706, 2000.
- [34] J. Crispim, M. Carreira, R. Castro, "Validation of PV electrical models against manufacturers data and experimental results," *Proceedings of International Conference on Power Engineering, Energy and Electrical Drives*, pp. 556-561, 2007.
- [35] K. Hussein, I. Muta, T. Hoshino, M. Osakada, "Maximum PV power tracking: an algorithm for rapidly changing atmospheric conditions in generation," *IEE Proceedings-Transmission and Distribution*, vol. 142, no. 1, p. 59-64, 1995.
- [36] D. Goldberg, *Genetic Algorithms in Search, Optimisation and Machine Learning*, Addison-Wesley Publishing Company, 1989.
- [37] R. Rajabioun, "Cuckoo optimization algorithm," *Applied Soft Computing*, vol. 11, no. 8, pp. 5508-5518, 2011.